

Dynamic Sparse Training for Deep Reinforcement Learning

Ghada Sokar¹, Elena Mocanu², Decebal Constantin Mocanu^{1,2}, Mykola Pechenizkiy¹ and Peter Stone³

¹Eindhoven University of Technology, The Netherlands

²University of Twente, The Netherlands

³The University of Texas at Austin, Sony AI, United States

{g.a.z.n.sokar, m.pechenizkiy}@tue.nl, {e.mocanu, d.c.mocanu}@utwente.nl, pstone@cs.utexas.edu

Abstract

Deep reinforcement learning (DRL) agents are trained through trial-and-error interactions with the environment. This leads to a long training time for dense neural networks to achieve good performance. Hence, prohibitive computation and memory resources are consumed. Recently, learning efficient DRL agents has received increasing attention. Yet, current methods focus on accelerating *inference* time. In this paper, we introduce for the *first time* a dynamic sparse training approach for deep reinforcement learning to accelerate the *training* process. The proposed approach trains a *sparse* neural network from scratch and dynamically adapts its topology to the changing data distribution during training. Experiments on continuous control tasks show that our *dynamic sparse* agents achieve higher performance than the equivalent dense methods, reduce the parameter count and floating-point operations (FLOPs) by 50%, and have a faster learning speed that enables reaching the performance of dense agents with 40 – 50% reduction in the training steps¹.

1 Introduction

Deep reinforcement learning (DRL) has achieved remarkable success in many applications. The power of deep neural networks as function approximators allows RL agents to scale to environments with high-dimensional state and action spaces. This enables high-speed growth in the field and the rise of many methods that improve the performance and stability of DRL agents [Wang *et al.*, 2020]. While the achieved performance is impressive, a long training time is required to obtain this performance. For instance, it took more than 44 days to train a Starcraft II agent using 32 third-generation tensor processing units (TPUs) [Vinyals *et al.*, 2019]. The very long training time leads to high energy consumption and prohibitive memory and computation costs. In this paper, we

ask the following question: *Can we provide efficient DRL agents with less computation cost and energy consumption while maintaining superior performance?*

Few recent works attempt to accelerate the *inference* time of DRL agents via pruning [Livne and Cohen, 2020] or training a compact network under the guidance of a larger network (knowledge distillation) [Zhang *et al.*, 2019]. Despite the computational improvement achieved at inference, extensive computations throughout the training of *dense* networks are still consumed. Our goal is to accelerate the training process as well as the inference time of DRL agents.

The long training time of a DRL agent is due to two main factors: **(1)** the extensive computational cost of training deep neural networks caused by the very high number of network parameters [Jouppi *et al.*, 2017] and **(2)** the learning nature of a DRL agent in which its policy is improving through many trial-and-error cycles while interacting with the environment and collecting a large amount of data. In this paper, we introduce dynamic sparse training (DST) [Mocanu *et al.*, 2021; Hoefler *et al.*, 2021] in the DRL paradigm for the first time to address these two factors. Namely, we propose an efficient training approach that can be integrated with existing DRL methods. Our approach is based on training *sparse* neural networks from scratch with a fixed parameter count throughout training **(1)**. During training, the sparse topology is optimized via adaptation cycles to *quickly adapt* to the online changing distribution of the data **(2)**. Our training approach enables reducing memory and computation costs substantially. Moreover, the quick adaptation to the new samples from the improving policy during training leads to a faster learning speed.

In fact, the need for neural networks that can adapt, e.g., change their control policy dynamically as environmental conditions change, was broadly acknowledged by the RL community [Stanley, 2003]. Although prior works related to the automatic selection of function approximation based on neuroevolution exist [Heidrich-Meisner and Igel, 2009], perhaps the most connected in the spirit to our proposed method is a combination of NeuroEvolution of Augmenting Topologies (NEAT) [Stanley and Miikkulainen, 2002] and temporal difference (TD) learning (i.e., NEAT+Q [Whiteson and Stone, 2006]). Still, the challenge remains, and cutting-edge DRL algorithms do not account for the benefits of adaptive neural networks training yet.

Our contributions in this paper are as follows:

¹Code is available at: <https://github.com/GhadaSokar/Dynamic-Sparse-Training-for-Deep-Reinforcement-Learning>. Proceedings of the 31st International Joint Conference on Artificial Intelligence (IJCAI-22).

- The principles of dynamic sparse training are introduced in the deep reinforcement learning field for the first time.
- Efficient improved versions of two state-of-the-art algorithms, TD3 [Fujimoto *et al.*, 2018] and SAC [Haarnoja *et al.*, 2018a], are obtained by integrating our proposed DST approach with the original algorithms.
- Experimental results show that our training approach reduces the memory and computation costs of training DRL agents by 50% while achieving superior performance. Moreover, it achieves a faster learning speed, reducing the required training steps.
- Analysis insights demonstrate the promise of dynamic sparse training in advancing the field and allowing for DRL agents to be trained and deployed on low-resource devices (e.g., mobile phones, tablets, and wireless sensor nodes) where the memory and computation power are strictly constrained. See Appendix C for discussion.

2 Related Work

Sparsity in DRL. To the best of our knowledge, the current advance in deep reinforcement learning is achieved using *dense* neural networks. Few recent studies have introduced sparsity in DRL via pruning. PoPS [Livne and Cohen, 2020] first trains a dense teacher neural network to learn the policy. This dense teacher policy network guides the iterative pruning and retraining of a student policy network via knowledge distillation. In [Zhang *et al.*, 2019], the authors aim to accelerate the behavior policy network and reduce the time for sampling. They use a smaller network for the behavior policy and learn it simultaneously with a large dense target network via knowledge distillation. GST [Lee *et al.*, 2021] was proposed as an algorithm for weight compression in DRL training by simultaneously utilizing weight grouping and pruning. Some other works [Yu *et al.*, 2019; Vischer *et al.*, 2021] studied the existence of the lottery ticket hypothesis [Frankle and Carbin, 2018] in RL, which shows the presence of sparse subnetworks that can outperform dense networks when they are trained from scratch. Pruning dense networks increases the computational cost of the training process as it requires iterative cycles of pruning and retraining [Molchanov *et al.*, 2019a; Renda *et al.*, 2020; Molchanov *et al.*, 2019b; Chen *et al.*, 2021]. This work introduces the first efficient training algorithm for DRL agents that trains sparse neural networks directly from scratch and adapts to the changing distribution.

Dynamic Sparse Training (DST). DST is the class of algorithms that train sparse neural networks *from scratch* and jointly optimize the weights and the sparse topology during training. This direction aims to reduce the computation and memory overhead of training dense neural networks by leveraging the redundancy in the parameters (i.e., being overparametrized) [Denil *et al.*, 2013]. Efforts in this line of research are devoted to supervised and unsupervised learning. The first work in this direction was proposed by [Mocanu *et al.*, 2018]. They proposed a Sparse Evolutionary Training algorithm (SET) that dynamically changes the sparse connectivity during training based on the values of the connections.

The method achieves higher performance than dense models and static sparse neural networks trained from scratch. The success of the SET algorithm opens the path to many interesting DST methods that bring higher performance gain. These algorithms differ from each other in the way the sparse topology is adapted during training [Mostafa and Wang, 2019; Evci *et al.*, 2020; Dettmers and Zettlemoyer, 2019; Jayakumar *et al.*, 2020; Bellec *et al.*, 2018; Liu *et al.*, 2021b; Raihan and Aamodt, 2020; Yuan *et al.*, 2021]. DST demonstrated its success in other fields as well, such as feature selection [Atashgahi *et al.*, 2020], continual learning [Sokar *et al.*, 2021], ensembling [Liu *et al.*, 2021a], federated learning [Zhu and Jin, 2019], text classification and language modeling tasks [Liu *et al.*, 2021c], and adversarial training [Özdenizci and Legenstein, 2021].

In this work, we adopt the topological adaptation from the SET method in our proposed approach. The motivation is multifold. First, SET is simple yet effective; it achieves the same or even higher accuracy than dense models with high sparsity levels across different architectures (e.g., multi-layer perceptrons, convolutional neural networks, restricted Boltzmann machines). Second, unlike other DST methods that use the values of non-existing (masked) weights in the adaptation process, SET uses only the values of existing sparse connections. This makes SET truly sparse and memory-efficient [Liu *et al.*, 2020]. Finally, it does not need high computational resources for the adaptation process. It uses readily available information during the standard training. These factors are favorable for our goal to train efficient DRL agents suitable for real-world applications. We leave evaluating other topological adaptation strategies for future work.

3 Proposed Method

In this section, we describe our proposed method, which introduces dynamic sparse training for the DRL paradigm. Here, we focus on integrating our training approach with one of the state-of-the-art DRL methods; Twin Delayed Deep Deterministic policy gradient (TD3) [Fujimoto *et al.*, 2018]. We named our new approach Dynamic Sparse TD3 or “DS-TD3” for short. TD3 is a popular and efficient DRL method that offers good performance in many tasks [Joshi *et al.*, 2021; Shi *et al.*, 2020; Ye *et al.*, 2021; Woo *et al.*, 2020; Hou *et al.*, 2021]. Yet, our approach can be merged into other DRL algorithms as well. Appendix E shows the integration with soft actor-critic (SAC) [Haarnoja *et al.*, 2018a].

TD3 is an actor-critic method that addresses the overestimation bias in previous actor-critic approaches. In actor-critic methods, a policy π is known as the *actor*, and a state-value function Q is known as the *critic*. Target networks are used to maintain fixed objectives for the actor and critic networks over multiple updates. In short, TD3 limits the overestimation bias using a pair of critics. It takes the smallest value of the two critic networks to estimate the Q value to provide a more stable approximation. To increase the stability, TD3 proposed a delayed update of the actor and target networks. In addition, the weights of the target networks are slowly updated by the current networks by some proportion τ . *In this work*, we aim to dynamically train the critics and actor networks along with

their corresponding target networks from scratch with sparse neural networks to provide efficient DRL agents. In the rest of this section, we will explain our proposed DST approach for TD3. The full details are also provided in Algorithm 1.

Our proposed DS-TD3 consists of four main phases: sparse topology initialization, adaptation schedule, topological adaptation, and maintaining sparsity levels.

Sparse Topology Initialization (Algorithm 1 L1-L4). TD3 uses two critic networks ($Q_{\theta_1}, Q_{\theta_2}$) and one actor network (π_ϕ) parameterized by $\theta_1 = \{\theta_1^l\}_{l=1}^L$, $\theta_2 = \{\theta_2^l\}_{l=1}^L$, and $\phi = \{\phi^l\}_{l=1}^L$ respectively; where L is the number of layers in a network. We initialize each of the actor and critic networks with a sparse topology. Sparse connections are allocated in each layer between the hidden neurons at layer $l-1$ and layer l . We represent the locations of the sparse connections by a binary mask $M = \{M^l\}_{l=1}^L$. Following [Mocanu *et al.*, 2018], we use Erdős–Rényi random graph [Erdos *et al.*, 1960] to initialize a sparse topology in each layer l . Namely, the probability of a connection j in layer l is given by:

$$p(M^j) = \lambda^l \frac{n^l + n^{l-1}}{n^l \times n^{l-1}}, \quad (1)$$

where λ^l is a hyperparameter to control the sparsity level in layer l , and n^{l-1} and n^l are the neurons count in layers $l-1$ and l , respectively. $M^j \in \{0, 1\}$; a value of 1 means the existence of a weight in location j . We omit the index l from the mask and weight matrices for readability. A sparse topology is created in each layer for the actor and critic networks:

$$\begin{aligned} \phi &= \phi \odot M_\phi, \\ \theta_i &= \theta_i \odot M_{\theta_i}, \quad \forall i \in \{1, 2\}, \end{aligned} \quad (2)$$

where \odot is an element-wise multiplication operator and M_ϕ , M_{θ_1} , and M_{θ_2} are binary masks to represent the sparse weights in the actor and two critic networks, respectively. The initial sparsity level is kept fixed during the training.

The target policy and target critic networks are parameterized by ϕ' , θ'_1 , and θ'_2 , respectively. Initially, the target networks have the same sparse topology and the same weights as the current networks: $\phi' \leftarrow \phi$, $\theta'_1 \leftarrow \theta_1$, $\theta'_2 \leftarrow \theta_2$.

After the topological and weight initialization, the agent collects enough data before training using a purely exploratory policy. During training, for each time step, TD3 updates the pair of critics towards the minimum target value of actions selected by the target policy $\pi_{\phi'}$:

$$y = r + \gamma \min_{i=1,2} Q_{\theta'_i}(s', \pi_{\phi'}(s') + \epsilon), \quad (3)$$

where γ is the discounting factor, r is the current reward, s' is the next state, and $\epsilon \sim \text{clip}(\mathcal{N}(0, \tilde{\sigma}), -c, c)$ is the proposed clipped noise by TD3, defined by $\tilde{\sigma}$, to increase the stability; where c is the clipped value. As discussed, TD3 proposed to delay the update of the policy network to first minimize the error in the value network before introducing a policy update. Therefore, the actor network is updated every d steps with respect to Q_{θ_1} as shown in Algorithm 1 L17-L19.

During the weight optimization of the actor and critic networks, the values of the existing sparse connections are only updated (i.e., the sparsity level is kept fixed). The sparse

Algorithm 1 DS-TD3 ($\lambda^l, \eta, e, N, \tau, d$)

- 1: Initialize critic networks $Q_{\theta_1}, Q_{\theta_2}$ and actor network π_ϕ with sparse parameters θ_1, θ_2, ϕ with a sparsity level defined by λ^l :
 - 2: Create M_ϕ, M_{θ_1} , and M_{θ_2} with Erdős–Rényi graph
 - 3: $\theta_1 \leftarrow \theta_1 \odot M_{\theta_1}, \theta_2 \leftarrow \theta_2 \odot M_{\theta_2}, \phi \leftarrow \phi \odot M_\phi$
 - 4: Initialize target networks $\theta'_1 \leftarrow \theta_1, \theta'_2 \leftarrow \theta_2, \phi' \leftarrow \phi$
 - 5: Initialize replay buffer \mathcal{B}
 - 6: **for** $t = 1$ **to** T **do**
 - 7: Select action with exploration noise $a \sim \pi_\phi(s) + \epsilon$,
 - 8: $\epsilon \sim \mathcal{N}(0, \sigma)$ and observe reward r and new state s'
 - 9: Store transition tuple (s, a, r, s') in \mathcal{B}
 - 10: Sample mini-batch of N transitions from \mathcal{B}
 - 11: $\tilde{a} \leftarrow \pi_{\phi'}(s') + \epsilon, \quad \epsilon \sim \text{clip}(\mathcal{N}(0, \tilde{\sigma}), -c, c)$
 - 12: $y \leftarrow r + \gamma \min_{i=1,2} Q_{\theta'_i}(s', \tilde{a})$
 - 13: $\theta_i \leftarrow \text{argmin}_{\theta_i} \frac{1}{N} \sum (y - Q_{\theta_i}(s, a))^2$
 - 14: **if** $t \bmod e$ **then**
 - 15: $\theta_i \leftarrow \text{TopologicalAdaptation}(\theta_i, M_{\theta_i}, \eta)$ (Algo. 2)
 - 16: **end if**
 - 17: **if** $t \bmod d$ **then**
 - 18: Update ϕ by the deterministic policy gradient:
 - 19: $\nabla_\phi J(\phi) \leftarrow \frac{1}{N} \sum \nabla_a Q_{\theta_1}(s, a)|_{a=\pi_\phi(s)} \nabla_\phi \pi_\phi(s)$
 - 20: **if** $t \bmod e$ **then**
 - 21: $\phi \leftarrow \text{TopologicalAdaptation}(\phi, M_\phi, \eta)$ (Algo. 2)
 - 22: **end if**
 - 23: Update target networks:
 - 24: $\theta'_i \leftarrow \tau \theta_i + (1 - \tau) \theta'_i$
 - 25: $\phi' \leftarrow \tau \phi + (1 - \tau) \phi'$
 - 26: $\theta'_i \leftarrow \text{MaintainSparsity}(\theta'_i, \|\theta_i\|_0)$ (Algo. 3)
 - 27: $\phi' \leftarrow \text{MaintainSparsity}(\phi', \|\phi\|_0)$ (Algo. 3)
 - 28: **end if**
 - 29: **end if**
-

topologies of the networks are also optimized during training according to our proposed adaptation schedule.

Adaptation Schedule. The typical practice in DST methods applied in the supervised setting is to perform the dynamic adaptation of the sparse topology after each training epoch. However, this would not fit the RL setting directly due to its dynamic learning nature. In particular, an RL agent faces instability during training due to the lack of a true target objective. The agent learns through trial and error cycles, collecting the data online while interacting with the environment. Adapting the topology very frequently in this learning paradigm would limit the exploration of effective topologies for the data distribution and give a biased estimate of the current one. To address this point, we propose to delay the adaptation process and perform it every e time steps, where e is a hyperparameter. This would allow the newly added connections from the previous adaptation process to grow. Hence, it would also give better estimates of the connections with the least influence in the performance and an opportunity to explore other effective ones. Analysis of the effect of the adaptation schedule in the success of applying dynamic sparse training in the RL setting is provided in Section 4.2.

Topological Adaptation (Algorithm 2). We adopt the

Algorithm 2 Topological Adaptation ($\mathbf{X}, \mathbf{M}, \eta$)

```
1:  $c \leftarrow \eta \|\mathbf{X}\|_0$ 
2:  $c_p \leftarrow c/2$ ;  $c_n \leftarrow c/2$ 
3:  $\tilde{\mathbf{X}}^p \leftarrow \text{get\_}c_p\text{-th\_smallest\_positive}(\mathbf{X})$ 
4:  $\tilde{\mathbf{X}}^n \leftarrow \text{get\_}c_n\text{-th\_largest\_negative}(\mathbf{X})$ 
5:  $\mathbf{M}^j \leftarrow \mathbf{M}^j - \mathbb{1}[(0 < \mathbf{X}^j < \tilde{\mathbf{X}}^p) \vee (0 > \mathbf{X}^j > \tilde{\mathbf{X}}^n)]$ 
6: Generate  $c$  random integers  $\{x\}_1^c$ 
7:  $\mathbf{M}^j \leftarrow \mathbf{M}^j + \mathbb{1}[(j == x) \wedge (\mathbf{X}^j == 0)]$ 
8:  $\mathbf{X} \leftarrow \mathbf{X} \odot \mathbf{M}$ 
```

Algorithm 3 Maintain Sparsity (\mathbf{X}, k)

```
1:  $\tilde{\mathbf{X}} \leftarrow \text{Sort\_Descending}(|\mathbf{X}|)$ 
2:  $\mathbf{M}^j = \mathbb{1}[\|\mathbf{X}^j - \tilde{\mathbf{X}}^k \geq 0], \forall j \in \{1, \dots, \|\mathbf{X}\|_0\}$ 
3:  $\mathbf{X} = \mathbf{X} \odot \mathbf{M}$ 
```

adaptation strategy of the SET method [Mocanu *et al.*, 2018] in our approach. The sparse topologies are optimized according to our adaptation schedule. Every e steps, we update the sparse topology of the actor and critic networks. Here, we explain the adaptation process on the actor network as an example. The same strategy is applied for the critic networks.

The adaptation process is performed through a “drop-and-grow” cycle which consists of two steps. **The first step** is to *drop* a fraction η of the least important connections from each layer. This fraction is a subset (c_p) of the smallest positive weights and a subset (c_n) of the largest negative weights. Thus, the removed weights are the ones closest to zero. Let $\tilde{\phi}^p$ and $\tilde{\phi}^n$ be the c_p -th smallest positive and the c_n -th largest negative weights, respectively. The mask \mathbf{M}_ϕ is updated to represent the dropped connections as follows:

$$\mathbf{M}_\phi^j = \mathbf{M}_\phi^j - \mathbb{1}[(0 < \phi^j < \tilde{\phi}^p) \vee (0 > \phi^j > \tilde{\phi}^n)], \quad \forall j \in \{1, \dots, \|\phi\|_0\}, \quad (4)$$

where \mathbf{M}_ϕ^j is the element j in \mathbf{M}_ϕ , $\mathbb{1}$ is the indicator function, \vee is the logical OR operator, and $\|\cdot\|_0$ is the standard L_0 norm. **The second step** is to *grow* the same fraction η of removed weights in random locations from the non-existing weights in each layer. \mathbf{M}_ϕ is updated as follows:

$$\mathbf{M}_\phi^j = \mathbf{M}_\phi^j + \mathbb{1}[(j == x) \wedge (\phi^j == 0)], \quad \forall j \in \{1, \dots, \|\phi\|_0\}, \quad (5)$$

where x is a random integer generated from the discrete uniform distribution in the interval $[1, n^{(l-1)} \times (n^l)]$ and \wedge is the logical AND operator. The weights of the newly added connections are zero-initialized ($\phi = \phi \odot \mathbf{M}_\phi$).

Maintain Sparsity Level in Target Networks (Algorithm 3). TD3 delays the update of the target networks to be performed every d steps. In addition, the target networks are slowly updated by some proportion τ instead of making the target networks exactly match the current ones (Algorithm 1 L23-L25). These two points lead to a slow deviation of the sparse topologies of the target networks from current networks. Consequently, the slow update of the target networks by τ would slowly increase the number of non-zero connections in the target networks over time. *To address this*, after each update of the target networks, we prune the extra connections that make the total number of connections exceed the

initial defined one. We prune the extra weights based on their smallest magnitude. Assume we have to retain k connections. The target masks of the actor ($\mathbf{M}'_{\phi'}$) and critics ($\mathbf{M}'_{\theta'_1}, \mathbf{M}'_{\theta'_2}$) are calculated as follows:

$$\begin{aligned} \mathbf{M}'_{\phi'} &= \mathbb{1}[|\phi'^j| - \tilde{\phi}'^k \geq 0], \quad \forall j \in \{1, \dots, \|\phi'\|_0\}, \\ \mathbf{M}'_{\theta'_i} &= \mathbb{1}[|\theta'_i{}^j| - \tilde{\theta}'^k_i \geq 0], \quad \forall j \in \{1, \dots, \|\theta'_i\|_0\}, \quad \forall i \in \{1, 2\}, \end{aligned} \quad (6)$$

where $\tilde{\phi}'^k$ and $\tilde{\theta}'^k_i$ is the k -th largest magnitude in the actor and critics respectively, and $|\cdot|^j$ is the magnitude of element j in the matrix. The target networks are updated as follows:

$$\begin{aligned} \phi' &= \phi' \odot \mathbf{M}'_{\phi'}, \\ \theta'_i &= \theta'_i \odot \mathbf{M}'_{\theta'_i} \quad \forall i \in \{1, 2\}. \end{aligned} \quad (7)$$

4 Experiments and Results

In this section, we assess the efficiency of our proposed dynamic sparse training approach for the DRL paradigm and compare it to state-of-the-art algorithms. Experimental settings are provided in Appendix A.

Baselines. We compare our proposed DS-TD3 against the following baselines: (1) *TD3* [Fujimoto *et al.*, 2018], the original TD3 where dense networks are used for actor and critic models, (2) *Static-TD3*, a variant of TD3 where the actor and critic models are initialized with sparse neural networks which are kept fixed during training (i.e., there is no topological optimization), and (3) *SAC* [Haarnoja *et al.*, 2018b], a popular off-policy algorithm in which the policy is trained to maximize a trade-off between expected return and entropy which results in policies that explore better.

Benchmarks. We performed our experiments on MuJoCo continuous control tasks, interfaced through OpenAI Gym. We evaluate our proposed approach on five challenging environments (HalfCheetah-v3, Hopper-v3, Walker2d-v3, Ant-v3, and Humanoid-v3).

Metrics. We use multiple metrics to assess the efficiency of the studied DRL methods (Details are in Appendix B): (1) **Return** which is the standard metric used in DRL to measure the *performance* of an agent, (2) **Learning curve area (LCA)** which estimates the *learning speed* of a model (i.e., how quickly a model learns) [Chaudhry *et al.*, 2018] by measuring the area under the training curve of a method, (3) **Network size (#params)** which measures the *memory cost* via the number of network parameters, and (4) **Floating-point operations (FLOPs)** which estimate the *computational cost* required for training. It is the typical metric in the literature to compare a DST method against its dense counterpart (see Appendix B for discussion).

4.1 Results

Learning Behavior and Speed. Figure 1 shows the learning curve of studied methods. DS-TD3 has a much faster learning speed than the baselines, especially at the beginning of the training. After 40-50% of the steps, DS-TD3 can achieve the final performance of TD3. Static-TD3 does not have this favorable property which reveals the importance of optimizing the sparse topology during training to adapt

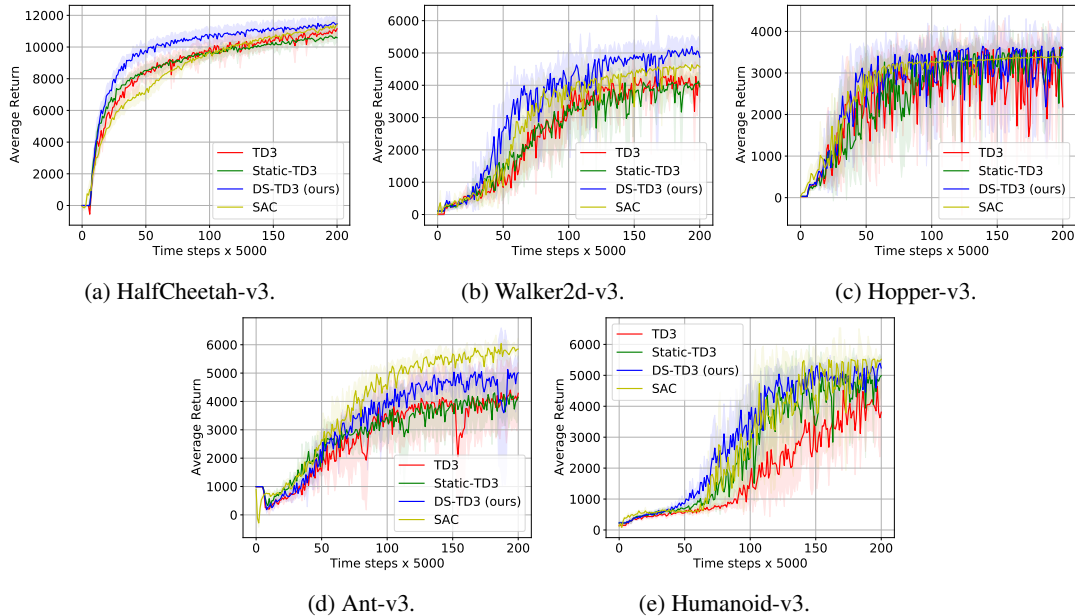


Figure 1: Learning curves of the studied algorithms on different continuous control tasks. The shaded region represents the standard deviation of the average evaluation over 5 runs.

Environment	TD3	Static-TD3	DS-TD3 (ours)	SAC
HalfCheetah-v3	1.7686	1.7666	1.9560	1.7297
Walker2d-v3	0.5264	0.5167	0.6956	0.6128
Hopper-v3	0.4788	0.4984	0.5435	0.5572
Ant-v3	0.5524	0.5807	0.6623	0.7969
Humanoid-v3	0.3635	0.5182	0.6089	0.5639

Table 1: Learning curve area (LCA) ($\times 5000$) of different methods.

to the incoming data. The learning behavior of DS-TD3 is also faster than SAC in all environments except one. Table 1 shows the learning curve area (LCA) of each method. DS-TD3 has higher LCA than TD3 and static-TD3 in all environments. It is also higher than SAC in three environments out of five. This metric is important to differentiate between two agents with similar final performance but very different LCA. **Performance.** Table 2 shows the average return (R) over the last 10 evaluations. DS-TD3 outperforms TD3 in all environments. Interestingly, it improves TD3 performance by 2.75%, 20.48%, 64.18%, 16.88%, and 37.51% on HalfCheetah-v3, Walker2d-v3, Hopper-v3, Ant-v3, and Humanoid-v3 respectively. Static-TD3 has a close performance to TD3 in most cases except for Humanoid-v3, where Static-TD3 outperforms TD3 by 30.98%. DS-TD3 has a better final performance than SAC in three environments.

4.2 Analysis

Memory and Computation Costs. We analyze the costs needed for the training process by calculating the FLOPs and #params for the actor and critics. We performed this analysis on Half-Cheetah-v3. #params for dense TD3 is 214784, which requires $1 \times (1.07e14)$ FLOPs to train. With our DS-TD3, we can find a much smaller topology that can effectively learn the policy and the function value, achieving

higher performance than TD3 with a sparsity level of 51%. This consequently reduces the number of required FLOPs to $0.49 \times (1.07e14)$.

Adaptation Schedule. We analyze the effect of the adaptation schedule on the performance. In particular, we ask how frequently the sparse topology should be adapted? We performed this analysis on HalfCheetah-v3. Figure 2a shows the learning curves of DS-TD3 using different adaptation schedules controlled by the hyperparameter e (Section 3). Adapting the topology very frequently (i.e., $e \in \{200, 500\}$) would not allow the connections to grow and learn in the dynamic changing nature of RL. The current adaptation process could remove some promising newly added connections from the previous adaptation process. This would be caused by a biased estimate of a connection’s importance as it becomes a factor of the length of its lifetime. Hence, the very frequent adaptation would increase the chance of replacing some promising topologies. With less frequent adaptation cycles, $e = 1000$ (the setting from the paper), DS-TD3 can learn faster and eventually achieves higher performance than other baselines. Giving the connections a chance to learn helps in having better estimates of the importance of the connections. Hence, it enables finding more effective topologies by replacing the least effective connections with ones that better fit the data. However, increasing the gap between every two consecutive adaptation processes to 2000 steps decreases the exploration speed of different topologies. As illustrated in the figure, DS-TD3 with $e = 2000$ has a close learning behavior and final performance to the dense TD3. Yet, it still offers a substantial reduction in memory and computation costs. This analysis reveals the importance of the adaptation schedule in the success of introducing DST to the DRL field.

Sparsity Level. We analyze the performance of our pro-

Method	HalfCheetah-v3	Walker2d-v3	Hopper-v3	Ant-v3	Humanoid-v3
TD3	11153.48±473.29	4042.36±576.57	2184.78±1224.14	4287.69±1080.88	3809.15±1053.40
Static-TD3	10583.84±307.03	3951.01±443.78	3570.88±43.71	4148.61±801.34	4989.47±546.32
DS-TD3 (ours)	11459.88±482.55	4870.57±525.33	3587.17±70.62	5011.56±596.95	5238.16±121.71
SAC	11415.23±357.22	4566.18±448.25	3387.36±148.73	5848.64±385.85	5518.61±97.03

Table 2: Average return (R) over the last 10 evaluations of 1 million time steps.

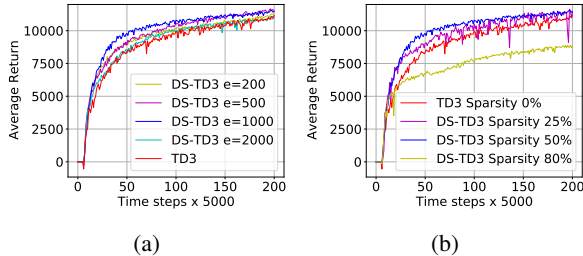


Figure 2: The learning curves of DS-TD3 on HalfCheetah-v3 using different adaptation schedules (a) and sparsity levels (b).

posed method using different sparsity levels. Figure 2b shows the learning curves of the dense TD3 and DS-TD3. By removing 25% of the connections and training the sparse topology dynamically using DS-TD3, we can achieve a faster learning speed and a performance increase of 2.11%. More interestingly, with a higher reduction in the size of the networks by 50%, we achieve a much faster learning speed. However, when the network has a very high sparsity level (i.e., 80%), it fails to learn effective representations for the reinforcement learning setting. Learning DRL agents using very high sparse networks is still an open-challenging task.

Learning Behavior and Speed. DRL agents learn through trial-and-error due to the lack of true labels. An agent starts training with samples generated from a purely exploratory policy, and new samples are drawn from the learning policy over time. Our results show that dynamic sparse agents have faster adaptability to the newly improved samples, thanks to the generalization ability of sparse neural networks [Hoefler *et al.*, 2021]. This leads to higher learning speed, especially at the beginning of the training. We hypothesize that dense neural networks, being over-parameterized, are more prone to memorize and overfit the inaccurate samples. A longer time is required to adapt to the newly added samples by the improved policy and forget the old ones.

To validate this hypothesis, we analyze the behavior of a dense TD3 agent when it starts training with samples generated from a learned policy instead of a purely exploratory one. We use two learned policies trained for 5×10^5 and 7×10^5 steps to draw the initial samples (see Appendix D). We performed this experiment on HalfCheetah-v3. As illustrated in Figure 3, the learning speed of DS-TD3 and TD3 becomes close to each other at the beginning. Afterward, DS-TD3 performs better than TD3 since the new samples are generated from the current learning policies. With initial samples drawn from more improved policy (Figure 3b), dense TD3 learns faster. It achieves higher performance than the baseline that starts learning with samples drawn from the policy

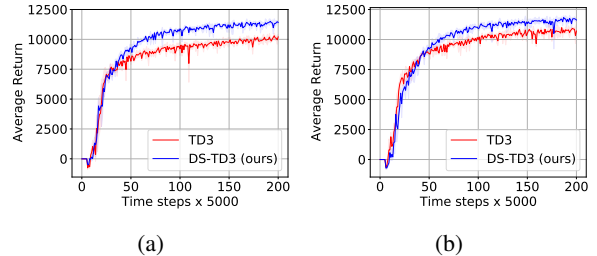


Figure 3: Learning curves of agents that start training with samples drawn from policies trained for 5×10^5 (a) and 7×10^5 steps (b).

trained for 5×10^5 steps (Figure 3a). On the other hand, DS-TD3 is more robust to over-fitting, less affected by the initial samples, and quickly adapt to the improved ones over time.

5 Conclusion

Introducing dynamic sparse training principles to the deep reinforcement learning field provides an efficient training process for DRL agents. Our dynamic sparse agents achieve higher performance than the state-of-the-art methods while reducing the memory and computation costs by 50%. Optimizing the sparse topology during training to adapt to the incoming data increases the learning speed. Our findings show the potential of dynamic sparse training in advancing the DRL field. This would open the path to efficient DRL agents that could be trained and deployed on low-resource devices where memory and computation are strictly constrained.

6 Acknowledgments

This material is partly based upon work supported by the Google Cloud Research Credits program.

References

- [Atashgahi *et al.*, 2020] Zahra Atashgahi, Ghada Sokar, Tim van der Lee, Elena Mocanu, Decebal Constantin Mocanu, Raymond Veldhuis, and Mykola Pechenizkiy. Quick and robust feature selection: the strength of energy-efficient sparse training for autoencoders. *arXiv preprint arXiv:2012.00560*, 2020.
- [Bellec *et al.*, 2018] Guillaume Bellec, David Kappel, Wolfgang Maass, and Robert Legenstein. Deep rewiring: Training very sparse deep networks. In *International Conference on Learning Representations*, 2018.
- [Chaudhry *et al.*, 2018] Arslan Chaudhry, Marc’Aurelio Ranzato, Marcus Rohrbach, and Mohamed Elhoseiny. Efficient lifelong learning with a-gem. In *International Conference on Learning Representations*, 2018.

- [Chen *et al.*, 2021] Tianlong Chen, Jonathan Frankle, Shiyu Chang, Sijia Liu, Yang Zhang, Michael Carbin, and Zhangyang Wang. The lottery tickets hypothesis for supervised and self-supervised pre-training in computer vision models. In *Proceedings of the IEEE/CVF Conference on Computer Vision and Pattern Recognition*, pages 16306–16316, 2021.
- [Denil *et al.*, 2013] Misha Denil, Babak Shakibi, Laurent Dinh, Marc’Aurelio Ranzato, and Nando de Freitas. Predicting parameters in deep learning. In *Proceedings of the 26th International Conference on Neural Information Processing Systems-Volume 2*, pages 2148–2156, 2013.
- [Dettmers and Zettlemoyer, 2019] Tim Dettmers and Luke Zettlemoyer. Sparse networks from scratch: Faster training without losing performance. *arXiv preprint arXiv:1907.04840*, 2019.
- [Erdos *et al.*, 1960] Paul Erdos, Alfréd Rényi, et al. On the evolution of random graphs. *Publ. Math. Inst. Hung. Acad. Sci.*, 5(1):17–60, 1960.
- [Evci *et al.*, 2020] Utku Evci, Trevor Gale, Jacob Menick, Pablo Samuel Castro, and Erich Elsen. Rigging the lottery: Making all tickets winners. In *International Conference on Machine Learning*, pages 2943–2952. PMLR, 2020.
- [Frankle and Carbin, 2018] Jonathan Frankle and Michael Carbin. The lottery ticket hypothesis: Finding sparse, trainable neural networks. In *International Conference on Learning Representations*, 2018.
- [Fujimoto *et al.*, 2018] Scott Fujimoto, Herke Hoof, and David Meger. Addressing function approximation error in actor-critic methods. In *International Conference on Machine Learning*, pages 1587–1596. PMLR, 2018.
- [Haarnoja *et al.*, 2018a] Tuomas Haarnoja, Aurick Zhou, Pieter Abbeel, and Sergey Levine. Soft actor-critic: Off-policy maximum entropy deep reinforcement learning with a stochastic actor. In *International Conference on Machine Learning*, pages 1861–1870. PMLR, 2018.
- [Haarnoja *et al.*, 2018b] Tuomas Haarnoja, Aurick Zhou, Kristian Hartikainen, George Tucker, Sehoon Ha, Jie Tan, Vikash Kumar, Henry Zhu, Abhishek Gupta, Pieter Abbeel, et al. Soft actor-critic algorithms and applications. *arXiv preprint arXiv:1812.05905*, 2018.
- [Heidrich-Meisner and Igel, 2009] Verena Heidrich-Meisner and Christian Igel. Neuroevolution strategies for episodic reinforcement learning. *Journal of Algorithms*, 64(4):152–168, 2009. Special Issue: Reinforcement Learning.
- [Hoefler *et al.*, 2021] Torsten Hoefler, Dan Alistarh, Tal Ben-Nun, Nikoli Dryden, and Alexandra Peste. Sparsity in deep learning: Pruning and growth for efficient inference and training in neural networks. *arXiv e-prints*, pages arXiv–2102, 2021.
- [Hooker, 2021] Sara Hooker. The hardware lottery. *Communications of the ACM*, 64(12):58–65, 2021.
- [Hou *et al.*, 2021] Yangyang Hou, Huajie Hong, Zhaomei Sun, Dasheng Xu, and Zhe Zeng. The control method of twin delayed deep deterministic policy gradient with re-birth mechanism to multi-dof manipulator. *Electronics*, 10(7):870, 2021.
- [Jayakumar *et al.*, 2020] Siddhant Jayakumar, Razvan Pascanu, Jack Rae, Simon Osindero, and Erich Elsen. Topkast: Top-k always sparse training. *Advances in Neural Information Processing Systems*, 33:20744–20754, 2020.
- [Joshi *et al.*, 2021] Tanuja Joshi, Shikhar Makker, Hariprasad Kodamana, and Harikumar Kandath. Application of twin delayed deep deterministic policy gradient learning for the control of transesterification process. *arXiv preprint arXiv:2102.13012*, 2021.
- [Jouppi *et al.*, 2017] Norman P Jouppi, Cliff Young, Nishant Patil, David Patterson, Gaurav Agrawal, Raminder Bajwa, Sarah Bates, Suresh Bhatia, Nan Boden, Al Borchers, et al. In-datacenter performance analysis of a tensor processing unit. In *Proceedings of the 44th annual international symposium on computer architecture*, pages 1–12, 2017.
- [Lee *et al.*, 2021] Juhyoung Lee, Sangyeob Kim, Sangjin Kim, Wooyoung Jo, and Hoi-Jun Yoo. Gst: Group-sparse training for accelerating deep reinforcement learning. *arXiv preprint arXiv:2101.09650*, 2021.
- [Liu *et al.*, 2020] Shiwei Liu, Decebal Constantin Mocanu, Amarsagar Reddy Ramapuram Matavalam, Yulong Pei, and Mykola Pechenizkiy. Sparse evolutionary deep learning with over one million artificial neurons on commodity hardware. *Neural Computing and Applications*, 33:2589–2604, 2020.
- [Liu *et al.*, 2021a] Shiwei Liu, Tianlong Chen, Zahra Atashgahi, Xiaohan Chen, Ghada Sokar, Elena Mocanu, Mykola Pechenizkiy, Zhangyang Wang, and Decebal Constantin Mocanu. Deep ensembling with no overhead for either training or testing: The all-round blessings of dynamic sparsity. *arXiv preprint arXiv:2106.14568*, 2021.
- [Liu *et al.*, 2021b] Shiwei Liu, Decebal Constantin Mocanu, Yulong Pei, and Mykola Pechenizkiy. Selfish sparse rnn training. In Marina Meila and Tong Zhang, editors, *Proceedings of the 38th International Conference on Machine Learning*, volume 139 of *Proceedings of Machine Learning Research*, pages 6893–6904. PMLR, 18–24 Jul 2021.
- [Liu *et al.*, 2021c] Shiwei Liu, Iftitahu Ni’mah, Vlado Menkovski, Decebal Constantin Mocanu, and Mykola Pechenizkiy. Efficient and effective training of sparse recurrent neural networks. *Neural Computing and Applications*, pages 1–12, 2021.
- [Livne and Cohen, 2020] Dor Livne and Kobi Cohen. Pops: Policy pruning and shrinking for deep reinforcement learning. *IEEE Journal of Selected Topics in Signal Processing*, 14(4):789–801, 2020.
- [Mocanu *et al.*, 2018] Decebal Constantin Mocanu, Elena Mocanu, Peter Stone, Phuong H Nguyen, Madeleine Gibescu, and Antonio Liotta. Scalable training of artificial neural networks with adaptive sparse connectivity inspired by network science. *Nature communications*, 9(1):1–12, 2018.

- [Mocanu *et al.*, 2021] Decebal Constantin Mocanu, Elena Mocanu, Tiago Pinto, Selima Curci, Phuong H Nguyen, Madeleine Gibescu, Damien Ernst, and Zita A Vale. Sparse training theory for scalable and efficient agents. In *Proceedings of the 20th International Conference on Autonomous Agents and MultiAgent Systems*, pages 34–38, 2021.
- [Molchanov *et al.*, 2019a] P Molchanov, S Tyree, T Karras, T Aila, and J Kautz. Pruning convolutional neural networks for resource efficient inference. In *5th International Conference on Learning Representations, ICLR 2017-Conference Track Proceedings*, 2019.
- [Molchanov *et al.*, 2019b] Pavlo Molchanov, Arun Mallya, Stephen Tyree, Iuri Frosio, and Jan Kautz. Importance estimation for neural network pruning. In *Proceedings of the IEEE/CVF Conference on Computer Vision and Pattern Recognition*, pages 11264–11272, 2019.
- [Mostafa and Wang, 2019] Hesham Mostafa and Xin Wang. Parameter efficient training of deep convolutional neural networks by dynamic sparse reparameterization. In *International Conference on Machine Learning*, pages 4646–4655. PMLR, 2019.
- [Özdenizci and Legenstein, 2021] Ozan Özdenizci and Robert Legenstein. Training adversarially robust sparse networks via bayesian connectivity sampling. In *International Conference on Machine Learning*, pages 8314–8324. PMLR, 2021.
- [Raihan and Aamodt, 2020] Md Aamir Raihan and Tor Aamodt. Sparse weight activation training. In H. Larochelle, M. Ranzato, R. Hadsell, M. F. Balcan, and H. Lin, editors, *Advances in Neural Information Processing Systems*, volume 33, pages 15625–15638. Curran Associates, Inc., 2020.
- [Renda *et al.*, 2020] Alex Renda, Jonathan Frankle, and Michael Carbin. Comparing rewinding and fine-tuning in neural network pruning. *arXiv preprint arXiv:2003.02389*, 2020.
- [Shi *et al.*, 2020] Qian Shi, Hak-Keung Lam, Chengbin Xuan, and Ming Chen. Adaptive neuro-fuzzy pid controller based on twin delayed deep deterministic policy gradient algorithm. *Neurocomputing*, 402:183–194, 2020.
- [Sokar *et al.*, 2021] Ghada Sokar, Decebal Constantin Mocanu, and Mykola Pechenizkiy. Spacenet: Make free space for continual learning. *Neurocomputing*, 439:1–11, 2021.
- [Stanley and Miikkulainen, 2002] Kenneth O Stanley and Risto Miikkulainen. Evolving neural networks through augmenting topologies. *Evolutionary computation*, 10(2):99–127, 2002.
- [Stanley, 2003] Kenneth O. Stanley. Evolving adaptive neural networks with and without adaptive synapses. In *In Proceedings of the 2003 Congress on Evolutionary Computation (CEC 2003)*, pages 2557–2564. Press, 2003.
- [Tandon, 2018] Pranjal Tandon. Pytorch implementation of soft actor critic, 2018.
- [Vinyals *et al.*, 2019] Oriol Vinyals, Igor Babuschkin, Wojciech M Czarnecki, Michaël Mathieu, Andrew Dudzik, Junyoung Chung, David H Choi, Richard Powell, Timo Ewalds, Petko Georgiev, et al. Grandmaster level in starcraft ii using multi-agent reinforcement learning. *Nature*, 575(7782):350–354, 2019.
- [Vischer *et al.*, 2021] Marc Aurel Vischer, Robert Tjarko Lange, and Henning Sprekeler. On lottery tickets and minimal task representations in deep reinforcement learning. *arXiv preprint arXiv:2105.01648*, 2021.
- [Wang *et al.*, 2020] Hao-nan Wang, Ning Liu, Yi-yun Zhang, Da-wei Feng, Feng Huang, Dong-sheng Li, and Yi-ming Zhang. Deep reinforcement learning: a survey. *Frontiers of Information Technology & Electronic Engineering*, pages 1–19, 2020.
- [Whiteson and Stone, 2006] Shimon Whiteson and Peter Stone. Evolutionary function approximation for reinforcement learning. *Journal of Machine Learning Research*, 7:877–917, May 2006.
- [Woo *et al.*, 2020] Jong Ha Woo, Lei Wu, Jong-Bae Park, and Jae Hyung Roh. Real-time optimal power flow using twin delayed deep deterministic policy gradient algorithm. *IEEE Access*, 8:213611–213618, 2020.
- [Ye *et al.*, 2021] Yujian Ye, Dawei Qiu, Huiyu Wang, Yi Tang, and Goran Strbac. Real-time autonomous residential demand response management based on twin delayed deep deterministic policy gradient learning. *Energies*, 14(3):531, 2021.
- [Yu *et al.*, 2019] Haonan Yu, Sergey Edunov, Yuandong Tian, and Ari S Morcos. Playing the lottery with rewards and multiple languages: lottery tickets in rl and nlp. *arXiv preprint arXiv:1906.02768*, 2019.
- [Yuan *et al.*, 2021] Geng Yuan, Xiaolong Ma, Wei Niu, Zhengang Li, Zhenglun Kong, Ning Liu, Yifan Gong, Zheng Zhan, Chaoyang He, Qing Jin, et al. Mest: Accurate and fast memory-economic sparse training framework on the edge. *Advances in Neural Information Processing Systems*, 34, 2021.
- [Zhang *et al.*, 2019] Hongjie Zhang, Zhuocheng He, and Jing Li. Accelerating the deep reinforcement learning with neural network compression. In *2019 International Joint Conference on Neural Networks (IJCNN)*, pages 1–8. IEEE, 2019.
- [Zhou *et al.*, 2020] Aojun Zhou, Yukun Ma, Junnan Zhu, Jianbo Liu, Zhijie Zhang, Kun Yuan, Wenxiu Sun, and Hongsheng Li. Learning n: M fine-grained structured sparse neural networks from scratch. In *International Conference on Learning Representations*, 2020.
- [Zhu and Jin, 2019] Hangyu Zhu and Yaochu Jin. Multi-objective evolutionary federated learning. *IEEE Transactions on Neural Networks and Learning Systems*, 31(4):1310–1322, 2019.

A Experimental Details

For a direct comparison with the TD3 algorithm, we follow the same setting as in [Fujimoto *et al.*, 2018]. We use multi-layer perceptrons for the actor and critics networks with two hidden layers of 256 neurons and a ReLU activation function. A Tanh activation is applied to the output layer of the actor network. Sparse connections are allocated in the first two layers for all networks while the output layer is dense. We use λ^2 of 64 for all environments. In contrast, λ^1 varies across environments because it depends on each environment’s state and action dimensions. We use λ^1 of 7 for HalfCheetah-v3, Hopper-v3, and Walker2d-v3. For Ant-v3 and Humanoid-v3, we use λ^1 of 40 and 61, respectively. The same sparsity levels are used for Static-TD3.

We adapt the sparse connections every e time steps, with $e = 1000$. A fraction of the sparse connections η is adapted with $\eta = 0.05$. The networks are trained using Adam optimizer with a learning rate of 0.001 and a weight decay of 0.0002. The networks are trained with mini-batches (N) of 100, sampled uniformly from a replay buffer containing the entire history of the agent.

Following the TD3 algorithm [Fujimoto *et al.*, 2018], we added noise of $\epsilon \sim \mathcal{N}(0, 0.2)$ to the actions chosen by the target actor network and clipped to $(-0.5, 0.5)$. The actor and target networks are updated every 2 steps ($d = 2$). The τ used for updating the target networks equals 0.005. A purely exploratory policy is used for the first 25000 time steps, then an off-policy exploration strategy is used with Gaussian noise of $\mathcal{N}(0, 0.1)$ added to each action.

The hyperparameters for the dynamic sparse training ($\lambda^1, \lambda^2, \eta, e$) are selected using random search. Each environment is run for 1 million time steps with evaluations every 5000 time steps, where each evaluation reports the average return over 10 episodes with no exploration noise. LCA is calculated using the average return computed every 5000 time steps. Our results are reported over 5 seeds.

All models are implemented with PyTorch and trained on Nvidia GPUs. We use the official code from the authors of TD3 [Fujimoto *et al.*, 2018], which has an MIT license, to reproduce the results of TD3 with the above settings.

For SAC, we use the Pytorch implementation from [Tandon, 2018]. We follow the settings from the original paper [Haarnoja *et al.*, 2018a] with the same architecture used for TD3. The networks are trained using Adam optimizer with a learning rate of 0.0003 and mini-batches of 256. We use τ of 0.005 and a target update interval of 1. The models are trained for 1M steps.

B Evaluation Metrics

In this appendix, we explain the details of the metrics used to assess the performance of our proposed method.

Return (R). The average return is the standard metric used in the RL research to measure the *performance* of an agent. The return is the sum of rewards (r) obtained in one episode of T steps. R is calculated as follows:

$$R = \sum_{t=1}^T r_t. \quad (8)$$

Learning curve area (LCA). This metric estimates the learning speed of a model. LCA measures the area under the training curve of a method. Intuitively, the higher learning curve, the faster the learner is. We adapt this metric from [Chaudhry *et al.*, 2018] to fit the reinforcement learning paradigm. LCA is calculated as follows:

$$LCA = \frac{1}{\Delta} \int_0^{\Delta} R(t) dt = \frac{1}{\Delta} \sum_{t=0}^{\Delta} R(t), \quad (9)$$

where Δ is the number of training steps and R is the average return.

Network size (#params). This metric estimates the *memory cost* consumed by an agent. The network size is estimated by the summation of the number of connections allocated in its layers as follows:

$$\#params = \sum_{l=1}^L \|\mathbf{W}^l\|_0, \quad (10)$$

where \mathbf{W}^l is the actual weights used in layer l , $\|\cdot\|_0$ is the standard L_0 norm, and L is the number of layers in the model. For sparse neural networks, $\|\mathbf{W}^l\|_0$ is controlled by its defined sparsity level for the model.

Floating-point operations (FLOPs). This metric estimates the *computational cost* of a method by calculating how many FLOPs are required for training. We follow the method described in [Evci *et al.*, 2020] to calculate the FLOPs. The FLOPs are calculated with the total number of multiplications and additions layer by layer in the network.

FLOPs is the typical used metric in the literature to compare a DST method against its dense counterpart. The motivation is twofold. First, it gives an unbiased estimate of the actual required number of operations since the running time would differ from one implementation to another. Second, more importantly, existing dynamic sparse training methods in the literature are currently prototyped using masks over dense weights to simulate sparsity [Hoeffler *et al.*, 2021]. This is because most deep learning specialized hardware is optimized for dense matrix operations. Therefore, the running time using these prototypes would not reflect the actual gain in memory and speed using a truly sparse network. Therefore, the FLOPs and network parameters are the current commonly used metrics to estimate the computation and memory costs respectively for sparse neural networks [Hoeffler *et al.*, 2021].

C Hardware and Software Support

As a joint community effort, research on sparsity is going into three parallel directions: First, hardware that supports sparsity. NVIDIA released NVIDIA A100, which supports a 50% fixed sparsity level [Zhou *et al.*, 2020]. Second, software libraries that support truly sparse implementations. Efforts have been started to be devoted to supervised learning [Liu *et al.*, 2020]. Third, algorithmic methods, our focus, that aim to provide approaches that achieve the same performance of dense models using sparse networks [Hoeffler *et al.*, 2021]. With the parallel efforts in the three directions, we would be able to actually provide faster, memory-efficient, and energy-efficient deep neural networks. This is further discussed in [Hooker, 2021; Mocanu *et al.*, 2021].

D Learning Behavior Analysis

To analyze the effect of the absence of true labels in the behavior of dense and dynamic sparse agents, we perform experiments in which an agent starts learning from samples drawn from a learned policy (Section 4.2). We test two learned policies with different performance to study how the quality of the initial samples affects the learning behavior. To this end, we train two dense policies using TD3 for 5×10^5 and 7×10^5 steps on Half-Cheetah-v3. Similarly, we train two sparse policies for the same time steps using DS-TD3. Instead of using a purely exploratory policy, we draw samples from the learned policies to fill the initial buffers for dense and dynamic sparse agents that learn from scratch.

As discussed in Section 4.2, the performance of dense DRL agents is more affected by the initial samples. The better the samples are, the higher performance is. On the other hand, dynamic sparse agents adapt quickly to the improving samples over time and are less affected by the quality of the initial samples.

E DS-SAC

In this appendix, we demonstrate that our proposed dynamic sparse training approach can be integrated with other state-of-the-art DRL methods. We use the soft actor-critic (SAC) method [Haarnoja *et al.*, 2018b] and name our improved version of it as Dynamic Sparse SAC or DS-SAC.

SAC is an off-policy algorithm that optimizes a stochastic policy. A key feature of this method is entropy regularization. The policy is trained to maximize a trade-off between expected return and entropy (a measure of randomness). Thus, the agent addresses the exploration-exploitation trade-off, which results in policies that explore better. Algorithm 4 shows our proposed DS-SAC. We integrated the four components of our approach (sparse topology initialization, adaptation schedule, topological adaptation, and maintain sparsity levels) into the original algorithm.

Tasks. We compared our proposed DS-SAC with SAC. We performed our experiments on five MuJoCo control tasks. Namely, we tested the following environments: HalfCheetah-v3, Hopper-v3, Walker2d-v3, Ant-v3, and Humanoid-v3.

Experimental settings. We follow the setting from the SAC method [Haarnoja *et al.*, 2018a]. All networks are multilayer perceptrons with two hidden layers of 256 neurons and a ReLU activation function. The networks are training with Adam optimizer and a learning rate of 0.0003. We use minibatches of 256. Each environment is run for 1 million steps. As DRL algorithms and their variants behave differently in various settings/environments, to cover a wider range of possible scenarios, we study here the case of hard target update where $\tau = 1$ [Haarnoja *et al.*, 2018a]. Following the original paper, target update interval= 1000. We use a temperature α of 0.2. Table 3 shows the value used for λ^1 and λ^2 to determine the sparsity levels for DS-SAC. We use e of 1000 and η of 0.1. The hyperparameters are selected using a random search. Our results are reported over 5 seeds.

Metrics. We used the same metrics discussed in Section 4 to assess the performance of our proposed method.

Algorithm 4 DS-SAC

```

1: Require:  $\lambda^1, \eta, e$ 
2: Create  $M_\phi, M_{\theta_1}$ , and  $M_{\theta_2}$  with Erdős–Rényi random
   graph with sparsity level  $\lambda^1$ 
3:  $\theta_1 \leftarrow \theta_1 \odot M_{\theta_1}, \theta_2 \leftarrow \theta_2 \odot M_{\theta_2}, \phi \leftarrow \phi \odot M_\phi$ 
4: Initialize target networks  $\bar{\theta}_1 \leftarrow \theta_1, \bar{\theta}_2 \leftarrow \theta_2$ 
5:  $\mathcal{D} \leftarrow \emptyset$  // Initialize an empty replay pool
6: for each iteration do
7:   for each environment step do
8:      $a_t \sim \pi_\phi(a_t|s_t)$  // Sample action from the policy
9:      $s_{t+1} \sim p(s_{t+1}|s_t, a_t)$  // Sample transition from the
       environment
10:     $\mathcal{D} \leftarrow \mathcal{D} \cup \{(s_t, a_t, r(s_t, a_t), s_{t+1})\}$  // Store the tran-
       sition in the replay pool
11:   end for
12:   for each gradient step do
13:      $\theta_i \leftarrow \theta_i - \lambda_Q \hat{\nabla}_{\theta_i} J_Q(\theta_i)$  // Update Q-functions
14:     if  $t \bmod e$  then
15:        $\theta_i \leftarrow \text{TopologicalAdaptation}(\theta_i, M_{\theta_i}, \eta)$  (Algo.
         2)
16:     end if
17:      $\phi \leftarrow \phi - \lambda_\pi \hat{\nabla}_\phi J_\pi(\phi)$  // Update policy weights
18:     if  $t \bmod e$  then
19:        $\phi \leftarrow \text{TopologicalAdaptation}(\phi, M_\phi, \eta)$  (Algo. 2)
20:     end if
21:      $\bar{\theta}_i \leftarrow \tau \theta_i + (1 - \tau) \bar{\theta}_i$  // Update target network
22:      $\bar{\theta}_i \leftarrow \text{MaintainSparsity}(\bar{\theta}_i, \|\theta_i\|_0)$  (Algo. 3)
23:   end for
24: end for

```

Table 3: The value used for λ^1 and λ^2 in each environment for the DS-SAC algorithm.

Environment	λ^1	λ^2
HalfCheetah-v3	12	80
Walker2d-v3	12	80
Hopper-v3	7	20
Ant-v3	30	64
Humanoid-v3	61	64

Results. Figure 4 shows the learning behavior of DS-SAC and SAC. Consistent with our previous observations, DS-SAC learns faster, especially at the beginning of the training. The LCA of DS-SAC is higher than SAC for all environments, as shown in Table 4. DS-SAC outperforms the final performance of SAC for all environments except one where it achieves a very close performance to it, as illustrated in Table 5. Please note that the results of SAC are slightly different from the ones obtained in Section 4.1 as we study here the hard target update case of SAC [Haarnoja *et al.*, 2018b].

These experiments reveal that we can achieve gain in a DRL agent’s learning speed and performance while reducing its required memory and computation costs for training.

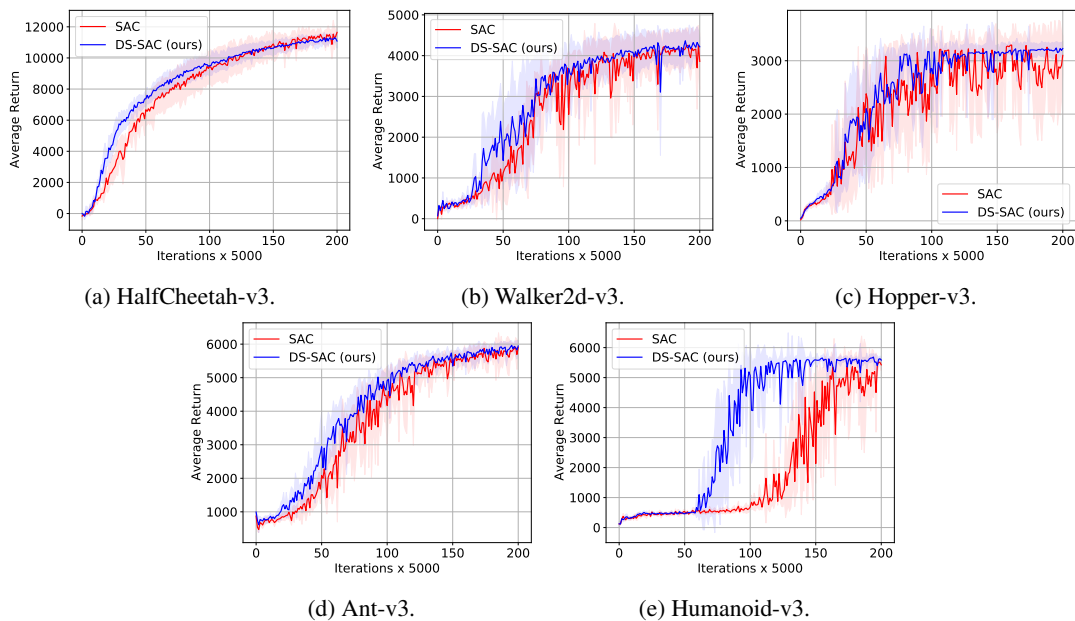


Figure 4: Learning curves of SAC and DS-SAC on different continuous control tasks. The shaded region represents the standard deviation of the average evaluation over 5 runs.

Table 4: Learning curve area (LCA) ($\times 5000$) of SAC and DS-SAC.

Environment	SAC	DS-SAC (ours)
HalfCheetah-v3	1.6229	1.7081
Walker2d-v3	0.5368	0.5906
Hopper-v3	0.4441	0.4875
Ant-v3	0.7504	0.8229
Humanoid-v3	0.3776	0.6777

Table 5: Average return over the last 10 evaluations of 1 million time steps using SAC and DS-SAC.

Environment	SAC	DS-SAC (ours)
HalfCheetah-v3	11645.12 \pm 425.585	11084.39 \pm 445.15
Walker2d-v3	3858.20 \pm 689.913	4216.77 \pm 236.23
Hopper-v3	3100.39 \pm 374.45	3229.39 \pm 135.82
Ant-v3	5899.30 \pm 197.15	5943.54 \pm 169.95
Humanoid-v3	5425.56 \pm 196.33	5584.64 \pm 109.40